INTERNATIONAL JOURNAL OF CLIMATOLOGY
Int. J. Climatol. (2013)
Published online in Wiley Online Library
(wileyonlinelibrary.com) DOI: 10.1002/joc.3765

RMetS
Royal Meteorological Society

Comparative analysis of the influence of solar radiation screen ageing on temperature measurements by means of weather stations

G. Lopardo,[a]* F. Bertiglia,[a] S. Curci,[b] G. Roggero[a] and A. Merlone[a]

[a] *INRiM, Istituto Nazionale di Ricerca Metrologica, Strada delle Cacce 73, 10135 Torino, Italy*
[b] *Climate Consulting S.r.l., Corso Sempione 6, 20154 Milano, Italy*

ABSTRACT: Solar radiation screens play a key role in automatic weather stations (AWS) performances. In this work, screen ageing effects on temperature measurements are examined. Paired temperature observations, traceable to national standards and with a well-defined uncertainty budget, were performed employing two naturally ventilated weather stations equipped with identical sensors and different only for their working time. Three different tests were carried out employing different aged AWSs: a 5-year-old AWS (AWS5) was compared with a new device (AWS0), a 1 year old (AWS1) was compared with both a 3 years old (AWS3) and a new one devices (AWS00). Due to solar and weather conditions exposure a degradation of the screen reflective coating is evident for the older AWSs (5 and 3 years old) and so a qualitative estimation of how different conditions of ageing affect the temperature drift was done. During the comparison 0 to 5 and 1 to 3-year-old screens, significant temperature differences were recorded at different times of the day. The differences, wider than the uncertainty amplitude, demonstrate a systematic effect. The temperature measured with the older screen is larger, and the maximum instantaneous difference was 1.63 °C (for 0–5 years comparison) in daytime hours. During night-time the two AWS's measure the same temperature (within the uncertainty amplitude). This behaviour, increasing with increasing solar radiation intensity and decreasing with increasing wind speed, is attributed to a radiative heating effect. The screen ageing has compromised the shield effectiveness introducing a significant change in the temperature evaluation. The experimental results of a further comparison, between 0- and 1-year-old screens, confirm the same conclusion showing a negligible ageing effect, within the uncertainty amplitude.

KEY WORDS radiation screen; ageing; weather station; air temperature; solar radiation; traceability; meteorological thermometer calibration

Received 14 December 2012; Revised 13 May 2013; Accepted 19 May 2013

1. Introduction

Despite constant improvements in sensors technology, accurate air temperature measurements are still a challenging task. Discussion among the scientific community is open aiming at defining methods and best practice for achieving representative atmospheric temperature records for meteorology and climatology. The representativeness of the place or area that the measuring stations cover require attention in the characterization, correction and possible minimization of influencing effects. Those effects are due to two main aspects: (1) influences of quantities other than temperature effecting the sensor reading, like sun or wind, humidity content etc. and (2) surrounding characteristics like presence of trees, building, ground coverage etc. In principle, the temperature reading of the thermometers embedded in the stations should be limited to the convection effect of the air surrounding the sensing element of the thermometer. The real measuring conditions are far from this ideal status, since contact and radiative contributions are always present. Modern automatic weather stations (AWS) are made to minimize contact heat exchange from the body of the station to the thermometers and are equipped with solar screens. The main function of thermometer screens is to prevent the solar direct and reflected radiation, shelters the sensor from inclement weather, and allows adequate airflow to ventilate the sensor (Van der Meulen and Brandsma, 2008). It follows that the thermometer screens should have a high reflectivity to minimize heating of the plates and subsequent warming of the air as it flows over the plates to the sensor. As a shield material, highly polished, non-oxidized metal or thermally insulating plastic-based materials are widely used (Aoshima *et al*., 2010), (WMO, 2008).

However, the screen reflective coatings are subjected to degradation in time. Due to solar and weather exposure, the screens age and their coatings colour changes from bright reflecting white to sort of light beige, compared to the new ones (Figure 1).

* Correspondence to: G. Lopardo, Istituto Nazionale di Ricerca Metrologica (INRiM), Strada delle Cacce 73, I-10135 Torino, Italy. E-mail: g.lopardo@inrim.it

Figure 1. Photograph of two of the AWSs used in the field trial. Left: 1 years old AWS (AWS1), in the right: 3-year-old device (AWS3).It is evident the colour variation of screen coating due to the ageing.

The ageing introduces a drift in the recorded temperature values and consequently inhomogeneities in series. A correct evaluation of this effect is fundamental to improve data quality and to avoid biases associated with shield ageing. The possibility to measure the temperature drift and eventually correct it could improve homogenization techniques in support of climate studies (Brunet *et al*., 2011).

In this work, we used an experimental approach to evaluate the magnitude of the screen ageing effect. We carried out in field paired temperature observations using old and new screens and estimated the differences. We employed naturally ventilated AWSs equipped with the same temperature sensors and the same type of round-shaped screens. The only difference consists in their working time: we compared five AWSs working for different years ranging from 0 to 5 years.

This work intends to give experimental evidence of the shield ageing effect on temperature records and represents the first step towards the evaluation of a more comprehensive uncertainty budget for surface air temperature including the ageing effect.

In the section 2 of this article, we describe the devices, the experimental condition and the calibration processes. In section 3, the temperature data recorded are analysed, finally, in section 4 measurement results are commented.

2. Data and methods

The temperature data were recorded at two experimental sites located in Torino and Milano, Italy, using instruments calibrated following two different procedures. This approach assures that the temperature differences found between AWSs equipped with old and new screens are effectively due to screen ageing effect being independent from calibration bias.

Besides, this comparative study allows estimating qualitatively how the different conditions of ageing affect the evaluated temperature. In the Torino site, we compared temperature data taken with two AWSs: a new device and a 5-year-old one. In the Milano site two tests were carried out, in the first we analysed temperature differences between 1- and 3-year-old AWS screens, in the second one the differences between a new device and 1-year-old screen

Table I. AWSs employed in the experiments and their working time.

	Employed in Milano site			Employed in Torino site	
	AWS00	AWS1	AWS3	AWS0	AWS5
Model	WXT520	WXT520	WXT520	WXT520	WXT510
Working time	New	2011	2009	New	2007

2.1. Automatic weather stations

The two sites were equipped with identical AWSs, model WXT520 manufactured by Vaisala, differing only in ageing and degradation of the screen reflective coating. In Table I, the devices employed and their ageing time are reported. Only the oldest weather station (AWS5) operating since 2007 is a WXT510; in the following years Vaisala replaced this model with WXT520. Both WXT520 and WXT510 are equipped with the same temperature sensors and the same type of round shaped screens.

The WXT weather transmitters (Figure 2) provide the measurement of atmospheric pressure, temperature and humidity by a 'PTU' module that contains separate sensors for the three quantities. The measurement principle is based on advanced RC oscillator and two reference capacitors against which the capacitance of the sensors is continuously measured. The PTU module includes:

- Capacitive silicon BAROCAP sensor for pressure measurement.
- Capacitive ceramic THERMOCAP sensor for air temperature.
- Capacitive thin film polymer HUMICAP sensor for humidity measurement.

The round-shaped multiplate screens are made of polycarbonate plus 20% glass fibre and the colour of the screens interior is black. The screens are naturally ventilated. Although, Vaisala provides standard configuration software, novel software, which directly reads and elaborates the string of data, was implemented (Meda *et al*., 2009). In this way it is possible to read only the parameters of interest and, hence, make the interrogation faster. The reading frequency can be set and data corrected using calibration curves.

2.2. Experimental set up

2.2.1. INRiM—Torino

The field experiment was performed between February and October 2012 at the meteorological equipment test

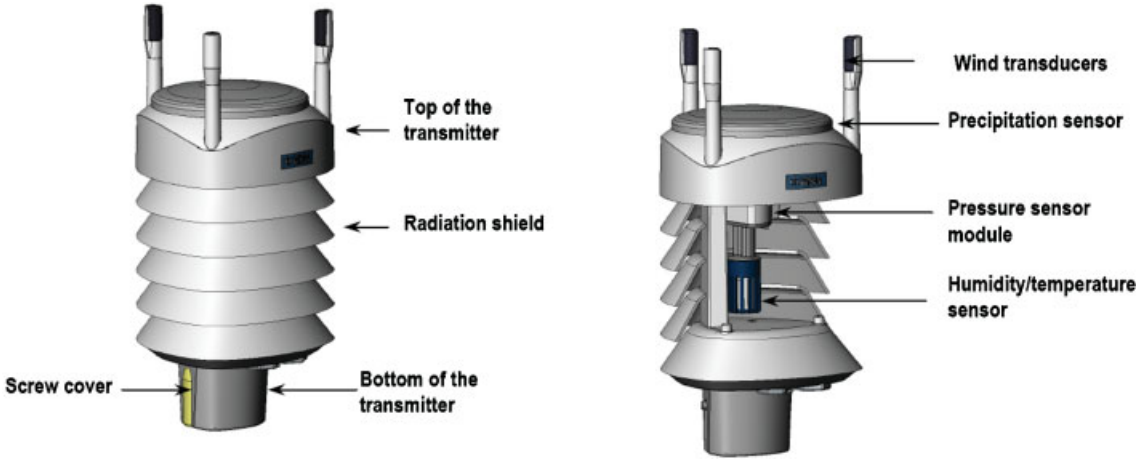

Figure 2. Vaisala weather transmitter. Left: front side with main components view. Right: cut away view with sensors location.

site of the INRiM in Torino (45°00′58.1″N/07°38′23.2″W at 242 m asl). The compared temperatures were recorded by the AWS0 (new device) and the AWS5 (5 years old). The two AWSs were located at 2 m above a flat terrain with short cut grass cover and sufficiently far from obstacles (building and trees). The nearness of the two AWS in less than 30 cm, allows very similar measurement conditions. Temperature was sampled by the two AWS's and archived instantaneously every 60 s and in the analysis a 600 s mean value was used. This averaging period was chosen to minimize local spatial differences (Van der Meulen and Brandsma, 2008). These procedures ensure that the differences found between the readings taken by the two AWSs can be associated to the reduced protection against solar radiation of the thermometer due to ageing of the AWS0 screen coating.

Wind speed and global solar radiation were measured by a weather station Davis Vantage Pro2™ Plus managed by Consiglio Nazionale delle Ricerche—Istituto di Ricerca per la Protezione Idrogeologica. The Davis station was located about 50 m from the AWSs position and at height of 3 m from the ground. Wind speed and solar radiation were recorded every 300 s.

2.2.2. *Meteorological observatory of the Duomo of Milano*

The field experiment was performed in May 2012 at the testing site of the Meteorological Observatory of the Duomo of Milano in the city center (45°27′50.98″N, 9°11′25.21″E at 122 m asl).

Two tests were carried out: in the first we analysed the temperature differences between the 1- and 3-year-old AWS screens (AWS1 *vs* AWS3), in the second between a new device and the 1-year-old screen (AWS00 *vs* AWS1).

The AWSs were located on the roof of a building 23 m high. Temperature data were recorded instantaneously every 2 s and in the analysis the mean of 300 records over 600 s was used.

Wind speed data were recorded by the Vaisala WINDCAP sensor integrated in the WXT510 AWSs.

Global solar radiation were measured by Kipp & Zonen CM5 sensor located near the AWSs at the same height. Wind speed and solar radiation were recorded every 600 s.

2.3. Calibration of the sensors

Independent calibrations of the sensors using different procedures were carried out in Milano and in Torino observations sites, in order to avoid calibration bias in the temperature measurements.

Global solar radiation and wind speed are here considered as influence quantities on air temperature measured values. Since this investigation is limited to relative temperature analysis not requiring absolute accurate values of temperature, wind speed and global solar radiation sensors were subjected only to manufacturer calibration.

2.3.1. *INRiM—Torino*

The two AWS's were calibrated against standards traceable to primary national ones, following *ad-hoc* calibration protocol defined at INRiM for meteorological sensors. This process assures traceability of temperature measurements and the evaluation of a complete calibration uncertainty budget.

The calibration was carried out in a special climate chamber manufactured at INRiM allowing the combined and simultaneous calibration of temperature, humidity and pressure used in the AWSs. This facility enables the evaluation of the impact of interfering quantities on individual calibration curves of sensors.

The temperature recorded by the AWSs was compared with a primary standard thermometer (Standard Platinum Resistance Thermometer with resistance of 25 Ω at 0 °C—SPRT25) in the temperature range covering the whole expected range of variability of the atmospheric temperature in the area (−20 °C to +50 °C). A calibration curve was calculated and applied in the acquisition software to correct the data collected.

The uncertainty budget was evaluated including different contribution: calibration uncertainty of the standard

Table II. Evaluation of calibration uncertainty for temperature recorded by each AWS.

Location	AWS	Calibration uncertainty of standard thermometer (°C)	Sensor resolution (°C)	Thermal stability of calibration chamber (°C)	Thermal uniformity of calibration chamber (°C)	Uncertainty on fit coefficients (°C)	Total calibration uncertainty (u_B) (°C)
INRiM	AWS0	0.001	0.029	0.01	0.14	0.1	0.17
	AWS5	0.001	0.029	0.01	0.14	0.09	0.17
Meteorological	AWS3	0.02	0.029	0.02	0.13	0.09	0.16
Observatory of	AWS1	0.02	0.029	0.03	0.16	0.07	0.18
Milano Duomo	AWS00	0.02	0.029	0.02	0.19	0.06	0.2

thermometer, resolution of the calibrated sensor, thermal uniformity and stability of the calibration chamber, uncertainty on fit coefficients. The total evaluated calibration uncertainty for the AWS0 and AWS5 was 0.17 °C (Table II).

The WXT510 sensors, during its lifetime, was recalibrated at intervals of about 1 year to evaluate and compensate possible drift due to sensors ageing or degradation (Meda *et al*., 2009).

2.3.2. Meteorological observatory of the Duomo of Milano

The temperature sensors calibration was separately carried out in a climatic test chamber manufactured by CTS using an independent procedure with respect to that adopted at INRiM.

Three second line work standards (Platinum thermometers with resistance of 100 Ω at 0 °C—PT100) were used for temperature comparisons. These last ones were calibrated against a secondary standard thermometer calibrated at INRiM using a comparator copper block located in the same climatic chamber. For more details about the calibration procedure see Curci *et al*., (2011). The calibration range was between −20 °C and +50 °C and the calibration curve was calculated and applied in the acquisition software to correct the data collected.

The calibration uncertainty budget for each AWS was evaluated including the same contributions described for the INRiM calibration. In Table II, the various calibration uncertainty contributions are summarized arising to a total uncertainty for AWS00 equal to 0.2 °C, 0.18 °C for AWS1, and 0.16 °C for AWS3.

2.4. Temperature differences uncertainty

The quantity of interest for this work is the difference (ΔT) between the temperatures measured by means of AWSs of different ages. According to the Guide to the expression of uncertainty in measurement (GUM) (BIPM, 2008), type A and type B uncertainties are evaluated for ΔT. Type A uncertainty is determined by statistical analysis, and type B by means other than statistical analysis. Since the coupled AWSs with different working times were kept in the same experimental conditions in terms of exposure, siting, data sampling etc., and the data were recorded at the same time, measurement type B uncertainties on their relative differences are considered negligible. Type B uncertainties are therefore due to calibration uncertainty and the type A contribution arise from the standard deviation of ΔT mean value evaluated in 600 s.

Table III. Type B, calibration uncertainty on temperature differences between AWS0 and AWS5 ($\Delta T_{\mathrm{AWS0-AWS5}} = T_{\mathrm{AWS0}} - T_{\mathrm{AWS5}}$), AWS1 and AWS3 ($\Delta T_{\mathrm{AWS1-AWS3}} = T_{\mathrm{AWS1}} - T_{\mathrm{AWS3}}$) and AWS00 and AWS1 ($\Delta T_{\mathrm{AWS00\text{-}AWS1}} = T_{\mathrm{AWS00}} - T_{\mathrm{AWS1}}$)[a].

AWS	Calibration uncertainty (u_B) (°C)	u_B ($\Delta T_{\mathrm{AWS0-AWS5}}$) (°C)	u_B ($\Delta T_{\mathrm{AWS1-AWS3}}$) (°C)	u_B ($\Delta T_{\mathrm{AWS00-AWS1}}$) (°C)
AWS0	0.17	0.24		
AWS5	0.17			
AWS3	0.16		0.24	
AWS1	0.18			0.27
AWS00	0.2			

[a] $u_B(\Delta T_{\mathrm{AWS0-AWS5}})$ is calculated as $u_B(\Delta T_{\mathrm{AWS0-AWS5}}) = \sqrt{[u_B(T_{\mathrm{AWS0}})]^2 + [u_B(T_{\mathrm{AWS5}})]^2}$ similarly for the other differences.

Table IV. Total calibration uncertainty on temperature differences between AWS0 and AWS5 ($\Delta T_{\mathrm{AWS0-AWS5}} = T_{\mathrm{AWS0}} - T_{\mathrm{AWS5}}$), AWS1 and AWS3 ($\Delta T_{\mathrm{AWS1-AWS3}} = T_{\mathrm{AWS1}} - T_{\mathrm{AWS3}}$) and AWS00 and AWS1 ($\Delta T_{\mathrm{AWS00\text{-}AWS1}} = T_{\mathrm{AWS00}} - T_{\mathrm{AWS1}}$).[a]

AWS	Type A uncertainty (u_A) (°C)	Type B uncertainty (u_B) (°C)	u_{tot}
$\Delta T_{\mathrm{AWS0-AWS5}}$	0.25	0.24	0.35
$\Delta T_{\mathrm{AWS1-AWS3}}$	0.25	0.24	0.35
$\Delta T_{\mathrm{AWS00-AWS1}}$	0.25	0.27	0.37

[a] $u_{\mathrm{tot}}(\Delta T_{\mathrm{AWS0-AWS5}})$ is evaluated as $u_{\mathrm{tot}}(\Delta T_{\mathrm{AWS0-AWS5}}) = \sqrt{\left[u_A(\Delta T_{\mathrm{AWS0-AWS5}})\right]^2 + \left[u_B(\Delta T_{\mathrm{AWS0-AWS5}})\right]^2}$ similarly for the other differences.

To better highlight the possible systematic effect due to solar screen ageing in the temperature measurements, for the expanded uncertainty a coverage factor $K = 1$ was chosen, corresponding to a confidence level of 68.27%.

For the temperature differences, the calibration uncertainty component is obtained summing in quadrature the calibration uncertainties of each AWS. The results, in the three experimental conditions (comparison 0–5 years, 1–3 years, and 0–1 years), are reported in Table III.

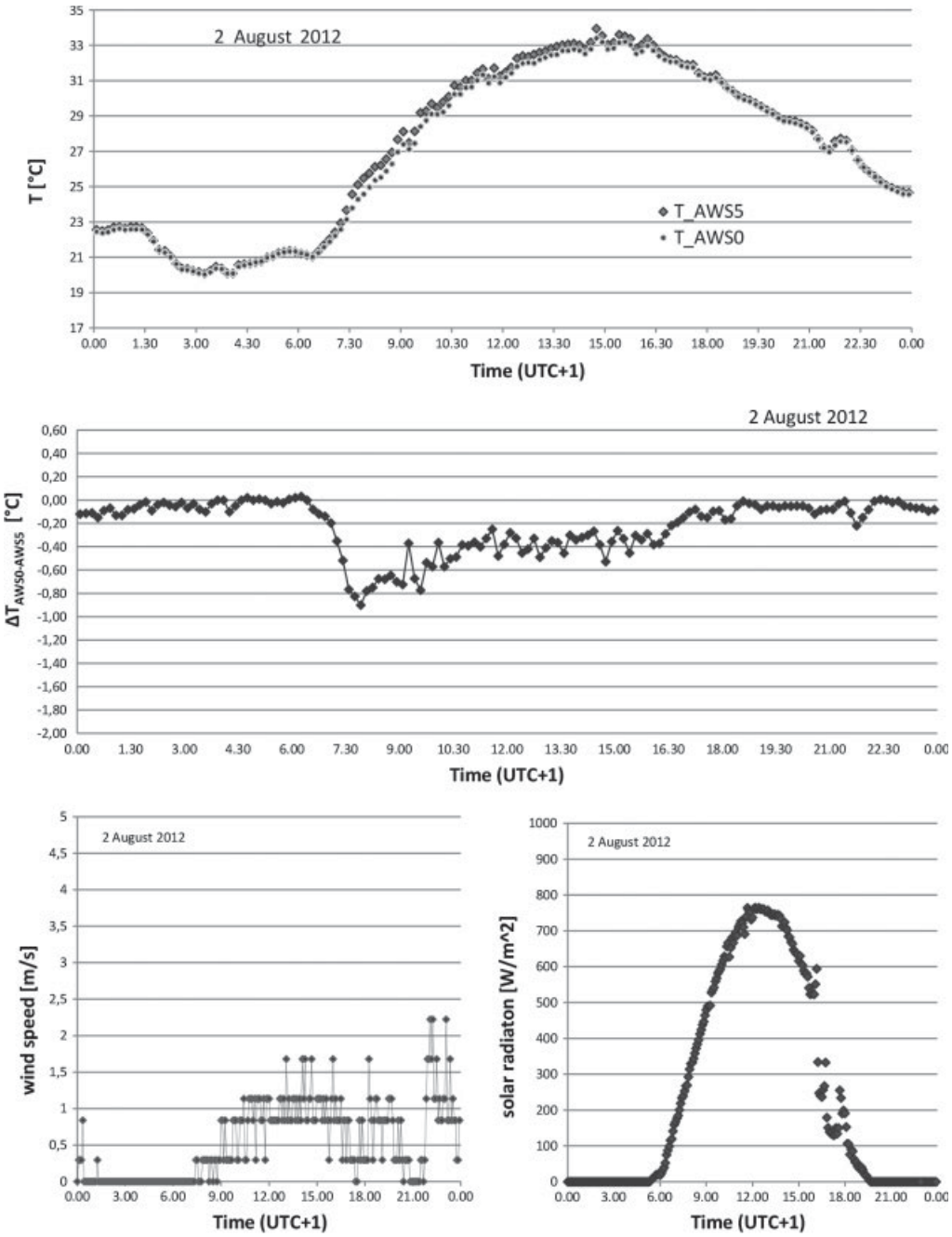

Figure 3. Temperature recorded by AWS0 and AWS5 for 2 August 2012. The figure also presents the temperature differences $\Delta T_{\mathrm{AWS0-AWS5}} = T_{\mathrm{AWS0}} - T_{\mathrm{AWS5}}$, wind speed, and solar radiation data.

The ΔT standard deviation, calculated in the three experimental conditions, is lower than 0.25 °C. To simplify the ΔT uncertainty evaluation we assume that, in the three experimental conditions, type A uncertainty ever equals 0.25 °C (maximum evaluated standard deviation).

Finally, the total uncertainty on ΔT is the quadratic sum of type A and type B uncertainties. As showed in Table IV, total uncertainty for both comparisons 0–5 years old ($\Delta T_{\mathrm{AWS0-AWS5}}$) and 1–3 years old ($\Delta T_{\mathrm{AWS1-AWS3}}$) is equal to 0.35 °C instead for the comparison 0–1 year old ($\Delta T_{\mathrm{AWS00-AWS1}}$) is equal to and 0.37 °C.

3. Results

Here, we discuss the observed temperature differences between the new and old AWS screens for a selection of representative days in the two sites. Different conditions of screen ageing are considered: 0–5 years (section 3.1), 1–3 years (section 3.2), and 0–1 years (section 3.3). Furthermore, we present summary statistics of temperature differences for daily and monthly data recorded in the 0–5 years comparison. The ageing effect on daily maximum, minimum, and mean temperatures is also analysed.

In following, we consider significant only the differences, bigger than 0.37 °C. This cut-off value is obtained

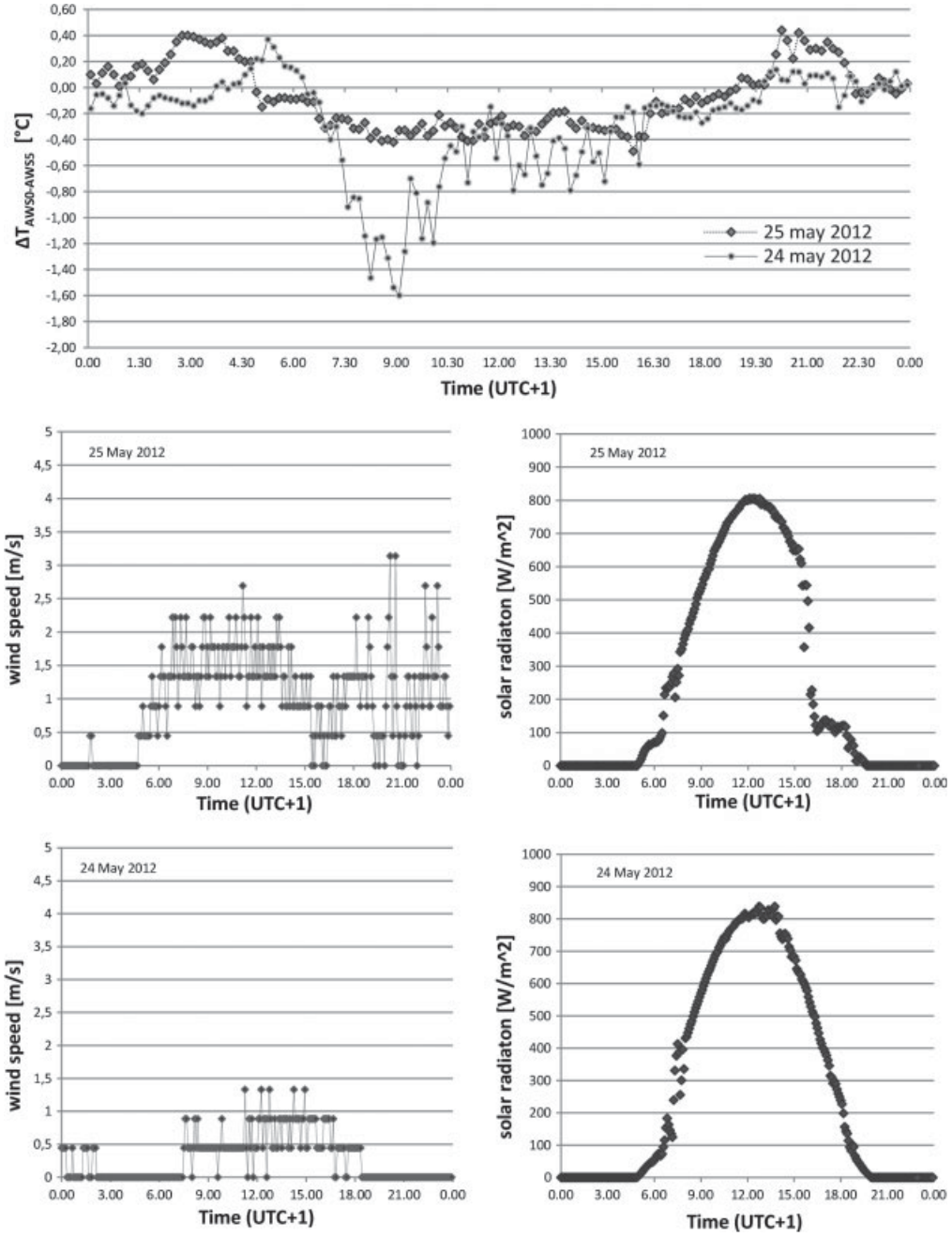

Figure 4. Temperature differences $\Delta T_{\mathrm{AWS0-AWS5}} = T_{\mathrm{AWS0}} - T_{\mathrm{AWS5}}$ for two selected days with different wind speed conditions. Wind speed and solar radiation are also reported.

selecting the maximum total uncertainty reported in Table IV.

3.1. Comparison of 0–5-year-old screens

In term of daily variation, Figure 3 shows the temperature data collected by AWS5 (T_{AWS5}) and AWS0 (T_{AWS0}) and their difference $\Delta T_{\mathrm{AWS0-AWS5}} = T_{\mathrm{AWS0}} - T_{\mathrm{AWS5}}$ on the 2 August 2012, global solar radiation and wind speed are reported too.

A negative $\Delta T_{\mathrm{AWS0-AWS5}}$ ($T_{\mathrm{AWS5}} > T_{\mathrm{AWS0}}$) is seen in the daytime hours, between 7:25 am and 4:00 pm (time UTC +1), the maximum $\Delta T_{\mathrm{AWS0-AWS5}}$ recorded in the day is $\Delta T^{*}_{\mathrm{AWS0-AWS5}} = -0.9\,^{\circ}\mathrm{C}$. Decreasing solar radiation intensity, in evening hours, the differences disappears.

It is well known that differences between (naturally ventilated) screens are most evident on clear days with low wind speed (Van der Meulen and Brandsma, 2008; Brandsma and Van der Meulen, 2008). Increasing wind speed and cloudiness causes these differences to dissipate.

The reduction of $\Delta T_{\mathrm{AWS0-AWS5}}$ for wind effect is reported in Figure 4.

In this figure are compared two clear days (24 and 25 May) with a similar mean solar radiation and different wind speed conditions. Mean solar radiation

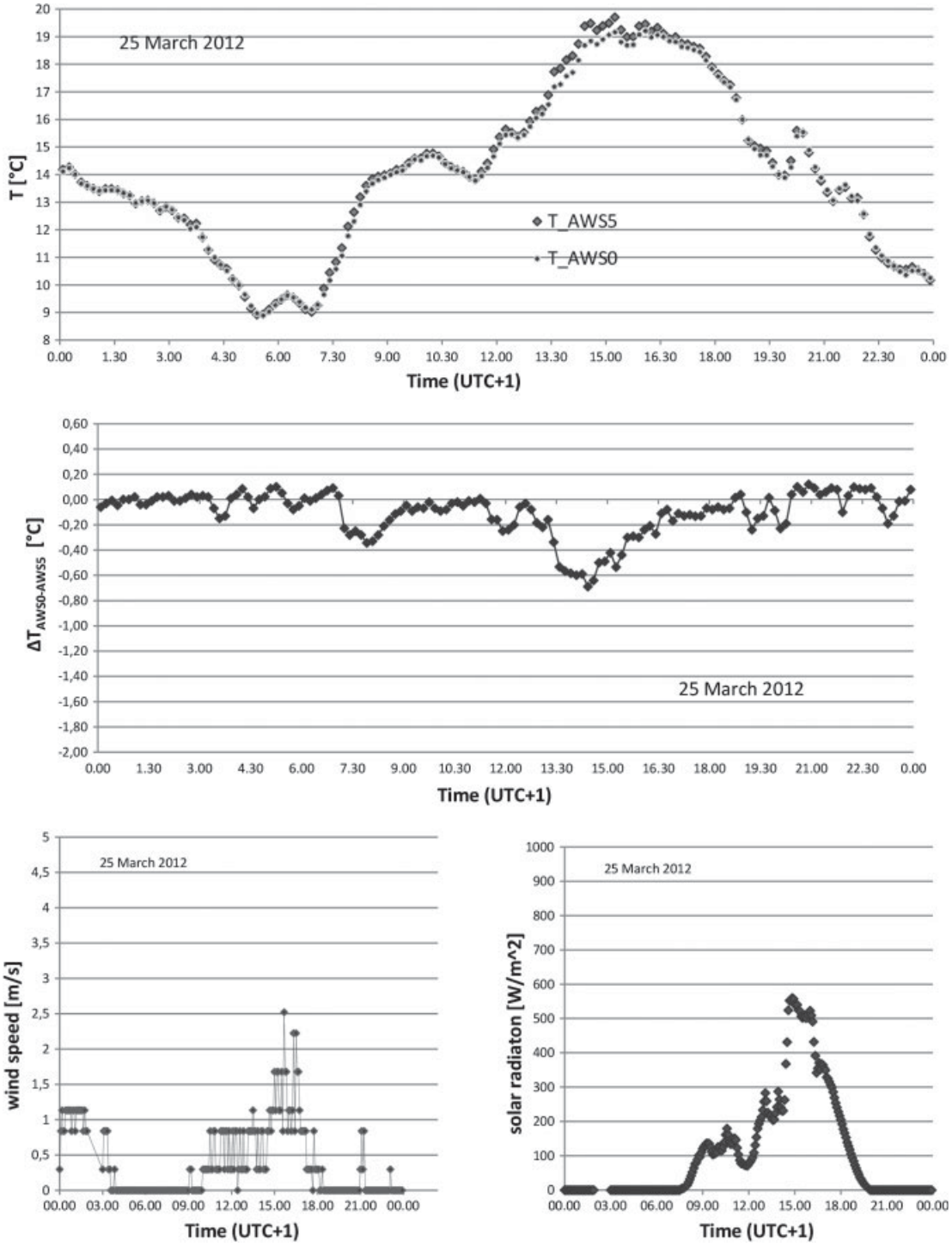

Figure 5. Temperature recorded by AWS0 and AWS5 for 25 March 2012. The figure also presents the temperature differences $\Delta T_{\mathrm{AWS0-AWS5}} = T_{\mathrm{AWS0}} - T_{\mathrm{AWS5}}$, wind speed, and solar radiation data.

on 24 May 2012 (S_{m}) was $S_{\mathrm{m}} = 292\,\mathrm{W\,m^{-2}}$ and mean wind speed (W_{m}) $W_{\mathrm{m}} = 0.52\,\mathrm{m\,s^{-1}}$, on 25 May 2012 $S_{\mathrm{m}} = 258\,\mathrm{W\,m^{-2}}$ and $W_{\mathrm{m}} = 1.42\,\mathrm{m\,s^{-1}}$. The mean wind speed was evaluated as mean value between 7:00 am and 5:00 pm that is the range in which the temperature differences occur. Though, during the considered experimental period, no high wind speed conditions were observed, the wind influence is evident. On 24 May the maximum temperature difference recorded was $\Delta T^{*}_{\mathrm{AWS0-AWS5}} = -1.60\,^{\circ}\mathrm{C}$, instead on 25 May 2012 were not measured significant differences (higher than cut-off value) between the new and the aged screens.

The cloudiness effect is well visible for 25 March 2012 (Figure 5) when for low solar radiation (during the morning hours) the two AWSs measure the same temperature within the uncertainty. The differences increase with solar radiation also if the wind appearing (between 3:00 and 4:30 pm) reduces the intensity of the effect.

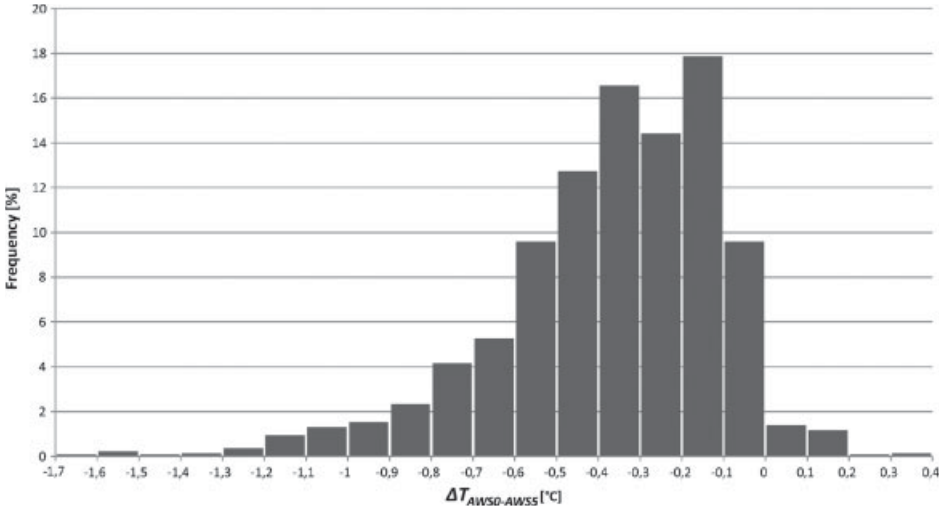

Figure 6. Histogram of the differences in the temperatures ($\Delta T_{\mathrm{AWS0-AWS5}}$) recorded by AWS0 ($T_{\mathrm{AWS0}}$) and AWS5 ($T_{\mathrm{AWS5}}$) in the observation period: $\Delta T_{\mathrm{AWS0-AWS5}} = T_{\mathrm{AWS0}} - T_{\mathrm{AWS5}}$.

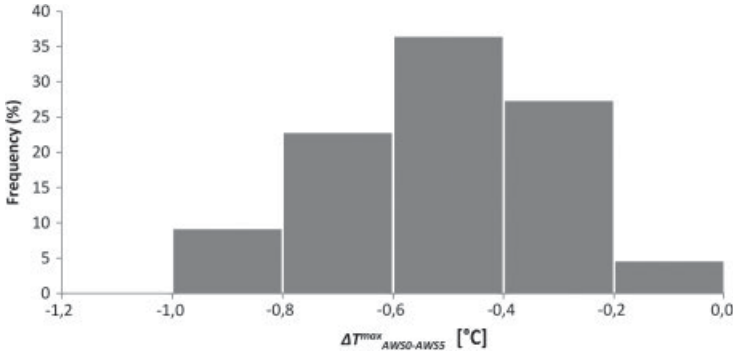

Figure 7. Histogram of the differences in the daily maximum temperatures $\left(\Delta T^{\mathrm{max}}_{\mathrm{AWS0-AWS5}}\right)$ recorded by AWS0 $\left(\Delta T^{\mathrm{max}}_{\mathrm{AWS0}}\right)$ and AWS5 $\left(\Delta T^{\mathrm{max}}_{\mathrm{AWS5}}\right)$ in the observation period: $\Delta T^{\mathrm{max}}_{\mathrm{AWS0-AWS5}} = T^{\mathrm{max}}_{\mathrm{AWS0}} - T^{\mathrm{max}}_{\mathrm{AWS5}}$.

In the histogram in Figure 6, we report the frequency distribution of all $\Delta T_{\mathrm{AWS0-AWS5}}$ observed in the central day time hours (7:00 am to 7:00 pm) in the experiment period. In the 38.8% of observations was observed a $\Delta T_{\mathrm{AWS0-AWS5}}$ higher than cut-off value. The mean value of the distribution is 0.32 °C.

Also daily maximum temperatures (T^{max}) are widely influenced by screen ageing effect. For the maximum daily temperature, the highest evaluated difference was −0.98 °C (27 May 2012). The histogram in Figure 7 reports the frequency distribution of $\Delta T^{\mathrm{max}}_{\mathrm{AWS0-AWS5}} = T^{\mathrm{max}}_{\mathrm{AWS0}} - T^{\mathrm{max}}_{\mathrm{AWS5}}$. In the 55% of days was observed a $\Delta T^{\mathrm{max}}_{\mathrm{AWS0-AWS5}}$ higher than cut-off value. The mean difference between the maximum temperatures was −0.46 °C

The graph in Figure 8 shows the mean values of $\Delta T_{\mathrm{AWS0\text{-}AWS5}}{}^{\mathrm{max}}$ recorded in the trial period for different atmospheric conditions. In overcast days, the mean difference between daily maximum temperatures was −0.36 °C instead in clear sky days becomes −0.56 °C. In windy days (mean wind speed higher than 1.4 m s^{-1}), the mean value was −0.43 °C, and −0.60 °C in lower wind conditions.

Also, monthly mean maximum temperatures are influenced by ageing effect. Table V shows the monthly mean differences between maximum temperatures recorded by AWS0 and AWS5 in the trial period.

The ageing effect does not influence the minimum and mean daily temperatures, because the minimum temperature occurs before the sunrise. For the mean temperature the evaluated differences are lower than −0.27 °C.

Table V. Monthly mean maximum temperature differences between AWS0 and AWS5 $\left(\Delta T^{\mathrm{max}}_{\mathrm{AWS0-AWS5}} = T^{\mathrm{max}}_{\mathrm{AWS0}} - T^{\mathrm{max}}_{\mathrm{AWS5}}\right)$.[a]

	Feb	Mar	Apr	May	June	July	Aug	Sep	Oct
$\overline{\Delta T}^{\mathrm{max}}_{\mathrm{AWS0-AWS5}}$	−0.52	−0.41	−0.36	−0.77	−0.56	−0.45	−0.39	−0.36	−0.35

[a] Observed period: February 2012 to October 2012.

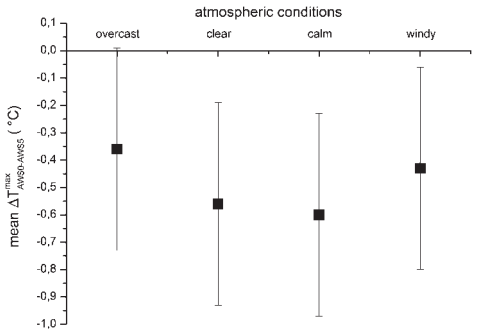

Figure 8. Mean value of differences in the daily maximum temperatures $(\Delta T^{\max}_{\mathrm{AWS0-AWS5}})$ recorded by AWS0 $(T^{\max}_{\mathrm{AWS0}})$ and AWS5 $(T^{\max}_{\mathrm{AWS5}})$ in the observation period for different atmospheric conditions: overcast and clear sky, windy and calm days. The uncertainty bar is also reported.

3.2. Comparison of 1 to 3-year-old screens

Figure 9 shows the temperature data collected by AWS3, T_{AWS3}, and AWS1, T_{AWS1} and their difference $\Delta T_{\mathrm{AWS1-AWS3}} = T_{\mathrm{AWS1}} - T_{\mathrm{AWS3}}$ for the 17 May 2012, a sunny day ($S_{\mathrm{m}} = 340\,\mathrm{W\,m^{-2}}$) with low wind speed conditions ($W_{\mathrm{m}} = 0.77\,\mathrm{m\,s^{-1}}$). The maximum difference recorded in the day was $\Delta T^{*}_{\mathrm{AWS1-AWS3}} = -0.6\,^{\circ}\mathrm{C}$.

The disappearing of any ageing effect for higher wind speed condition is showed in Figure 10 where a sunny windy day ($S_{\mathrm{m}} = 334\,\mathrm{W\,m^{-2}}$, $W_{\mathrm{m}} = 3.71\,\mathrm{m\,s^{-1}}$), 16 May 2012, was reported. No significant $\Delta T_{\mathrm{AWS1-AWS3}}$ was measured during the whole day.

This behaviour is confirmed also by the comparison in Figure 11 between values recorded on 16 May, the most windy day observed, and on 14 May 2012, with similar mean solar radiation $S_{\mathrm{m}} = 323.6\,\mathrm{W\,m^{-2}}$ and lower wind speed $W_{\mathrm{m}} = 0.75\,\mathrm{m\,s^{-1}}$. The 14 May the maximum temperature difference recorded was $\Delta T^{*}_{\mathrm{AWS1-AWS3}} = -0.52\,^{\circ}\mathrm{C}$.

Finally, as done in the previous section, in Figure 12 the cloudiness effect is reported for the 20 May 2012, resulting in negligible temperature differences.

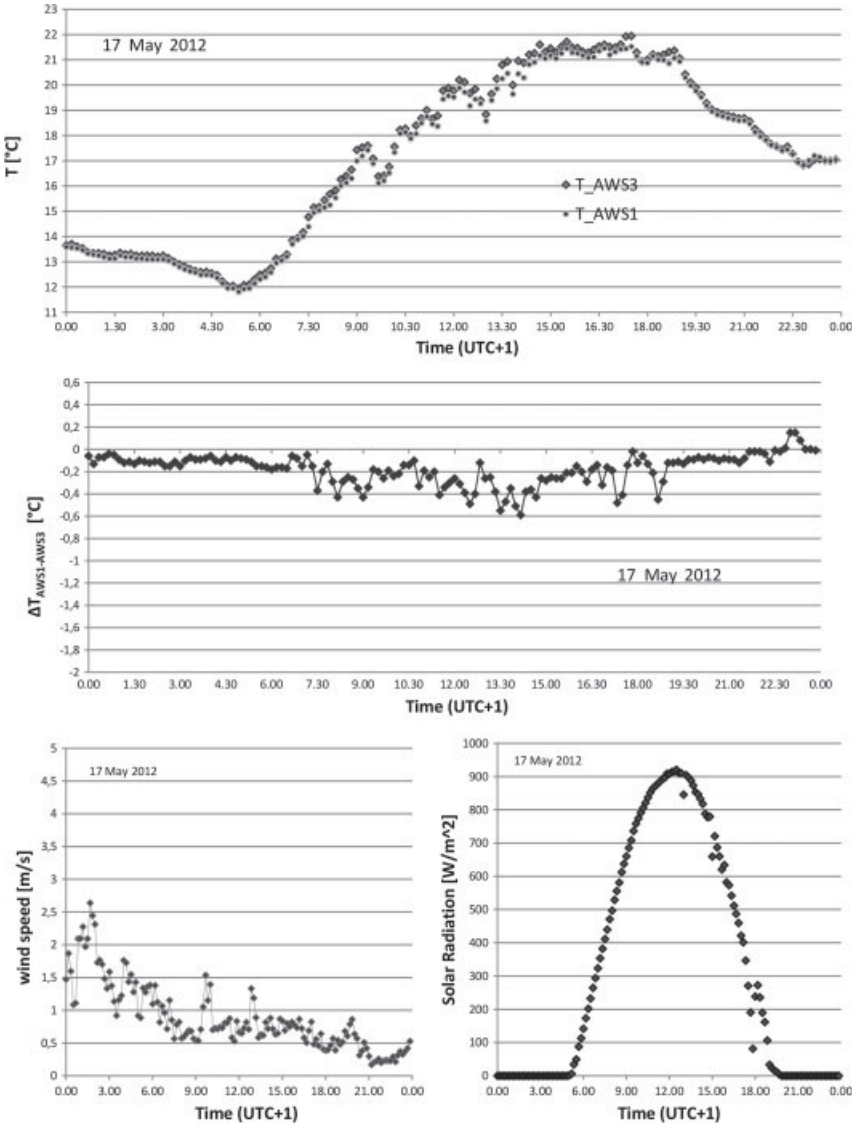

Figure 9. Temperature recorded by AWS1 and AWS3 for 17 May 2012. The figure also presents the temperature differences $\Delta T_{\mathrm{AWS1-AWS3}} = T_{\mathrm{AWS1}} - T_{\mathrm{AWS3}}$, wind speed, and solar radiation data.

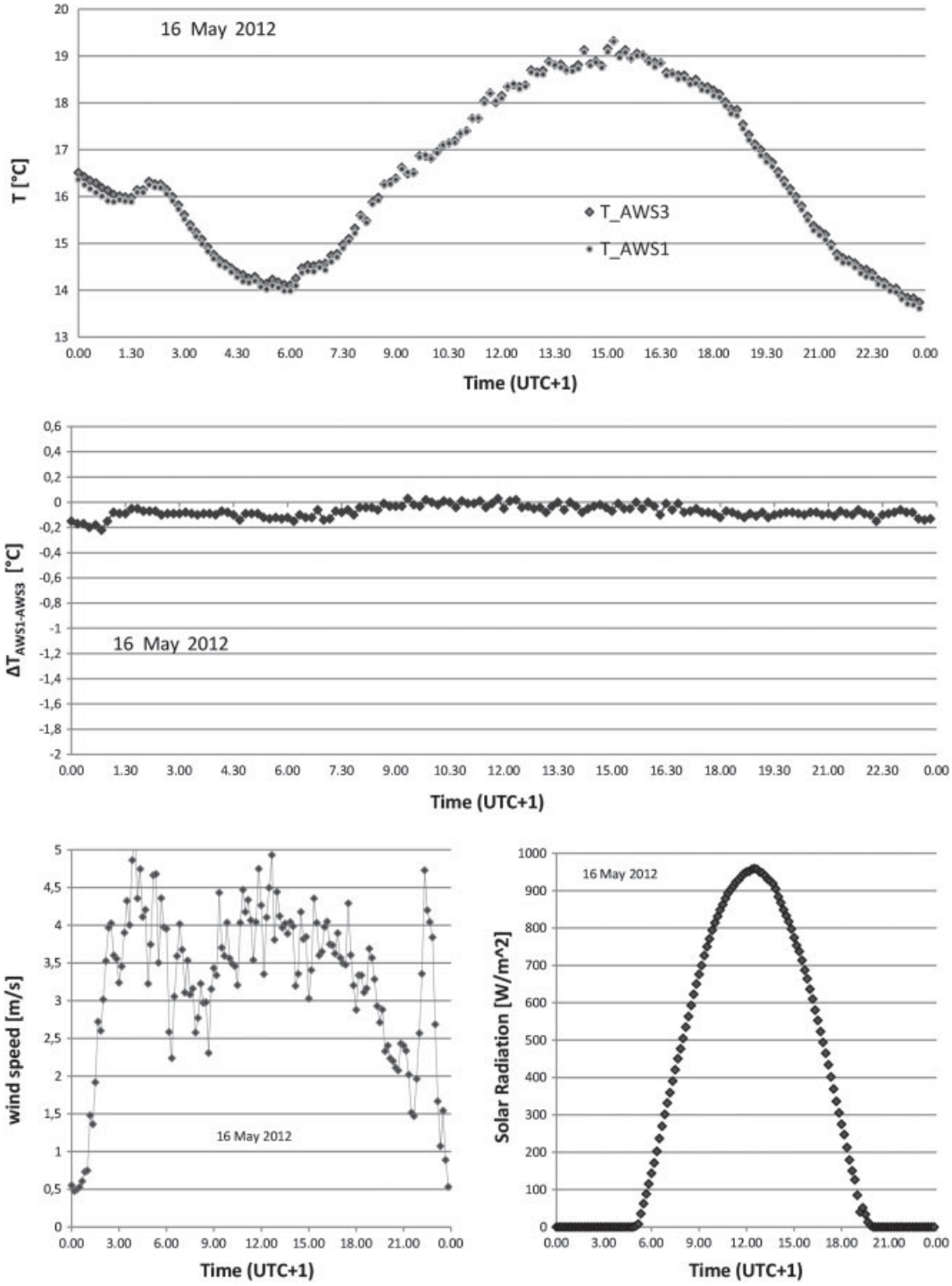

Figure 10. Temperature recorded by AWS1 and AWS3 for 16 May 2012. The figure also presents the temperature differences $\Delta T_{\mathrm{AWS1}-\mathrm{AWS3}} = T_{\mathrm{AWS1}} - T_{\mathrm{AWS3}}$, wind speed, and solar radiation data.

For the maximum daily temperature: the maximum evaluated difference was $-0.59\,^{\circ}$C (recorded on 18 May 2012), the mean value instead was $-0.49\,^{\circ}$C. The mean measured difference for the mean daily temperatures (evaluated between 7:00 am to 7:00 pm) was $-0.25\,^{\circ}$C.

3.3. Comparison of 0 to 1-year-old screens

During the observation period, the temperature data collected by AWS00 (T_{AWS00}), and AWS1 (T_{AWS1}) are within the uncertainty range, and the differences $\Delta T_{\mathrm{AWS00\text{-}AWS1}} = T_{\mathrm{AWS00}} - T_{\mathrm{AWS1}}$ are negligible. Figure 13 reports T_{AWS00}, T_{AWS1}, $\Delta T_{\mathrm{AWS00-AWS1}}$, wind speed, and mean solar radiation for the 23 May 2012.

3.4. Comment

The experiments carried out on the 0 to 5 and 1 to 3-year-old screens confirm the existence of shield ageing effect due to the degradation of the protective paint, in

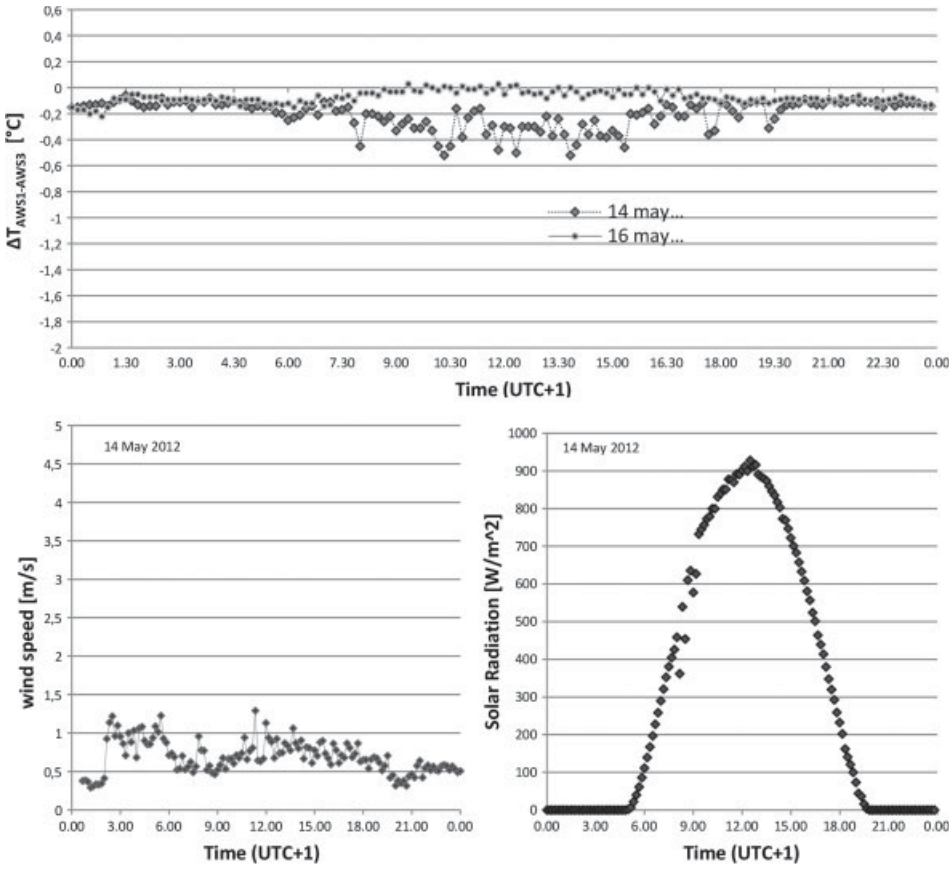

Figure 11. Temperature differences $\Delta T_{\mathrm{AWS1}-\mathrm{AWS3}} = T_{\mathrm{AWS1}} - T_{\mathrm{AWS3}}$ for two selected days with different wind speed conditions:16 and 14 May 2012. Wind speed and solar radiation conditions are also reported.

both cases. However, as expected, this effect is more evident comparing shields with higher working time apart. Figure 14 presents histograms of the $\Delta T^*_{\mathrm{AWS0}-\mathrm{AWS5}}$ and $\Delta T^*_{\mathrm{AWS1}-\mathrm{AWS3}}$ recorded in the observation periods. Values of $|\Delta T^*_{\mathrm{AWS0}-\mathrm{AWS5}}|$ higher than $|\Delta T^*_{\mathrm{AWS1}-\mathrm{AWS3}}|$ are evident.

In the case of 0 to 1-year-old screens the ageing effect is not present within the uncertainty cut-off value. We can conclude that the degradation of the AWS1 screen is not so critical. To see the effect, a longer solar exposition or exposition to more intense radiation is needed.

4. Discussion and conclusions

Paired temperature readings recorded by two sets of Vaisala AWSs were performed in two different experimental sites in Torino and Milano. In Torino site a new and 5-year-old AWS were employed, in Milano a new, a 1- and 3-year-old AWSs were used to evaluate 0–1 and 1–3 years of different ageing effect. All AWSs have the same technical characteristics and typology of sensors and screens. The only difference between AWSs is in the degradation of the screens protective coatings due to solar exposure during their lifetimes. The AWS3 and AWS5 aged and their coatings became light beige compared to the new screens of the AWS1, AWS0, and AWS00 (the last two AWSs were never used before the experiment here reported).

The AWS sensors, in both sites, were calibrated against national standards, following independent procedures and employing different calibration chambers. The temperature data reported in this article were corrected with calibration curves and the associated calibration uncertainty budget was evaluated.

The temperature measurements recorded by old and new screens were compared, in both sites, and significant differences were found when AWSs with higher working time apart are compared: 0–5 and 1–3 years old screens. The temperatures measured by the AWS5 (respectively AWS3) were larger than the AWS0 (AWS1). The maximum differences measured were $\Delta T^*_{\mathrm{AWS0}-\mathrm{AWS5}} = -1.63\,^{\circ}\mathrm{C}$ and $\Delta T^*_{\mathrm{AWS1}-\mathrm{AWS3}} = -0.73\,^{\circ}\mathrm{C}$. The maximum differences recorded in the comparison 0–5 years were always bigger than that in 1–3 years to demonstrate that the ageing effect depends by paints degradation degree. Instead, in the case 0 to 1-year-old screens temperature differences are not evident.

Analysing maximum daily temperatures, the mean difference in 0–5 years comparison was $-0.46\,^{\circ}\mathrm{C}$. Minimum daily temperatures are not impacted by ageing effect, instead for the mean daily temperature the evaluated differences were less than the calibration uncertainty.

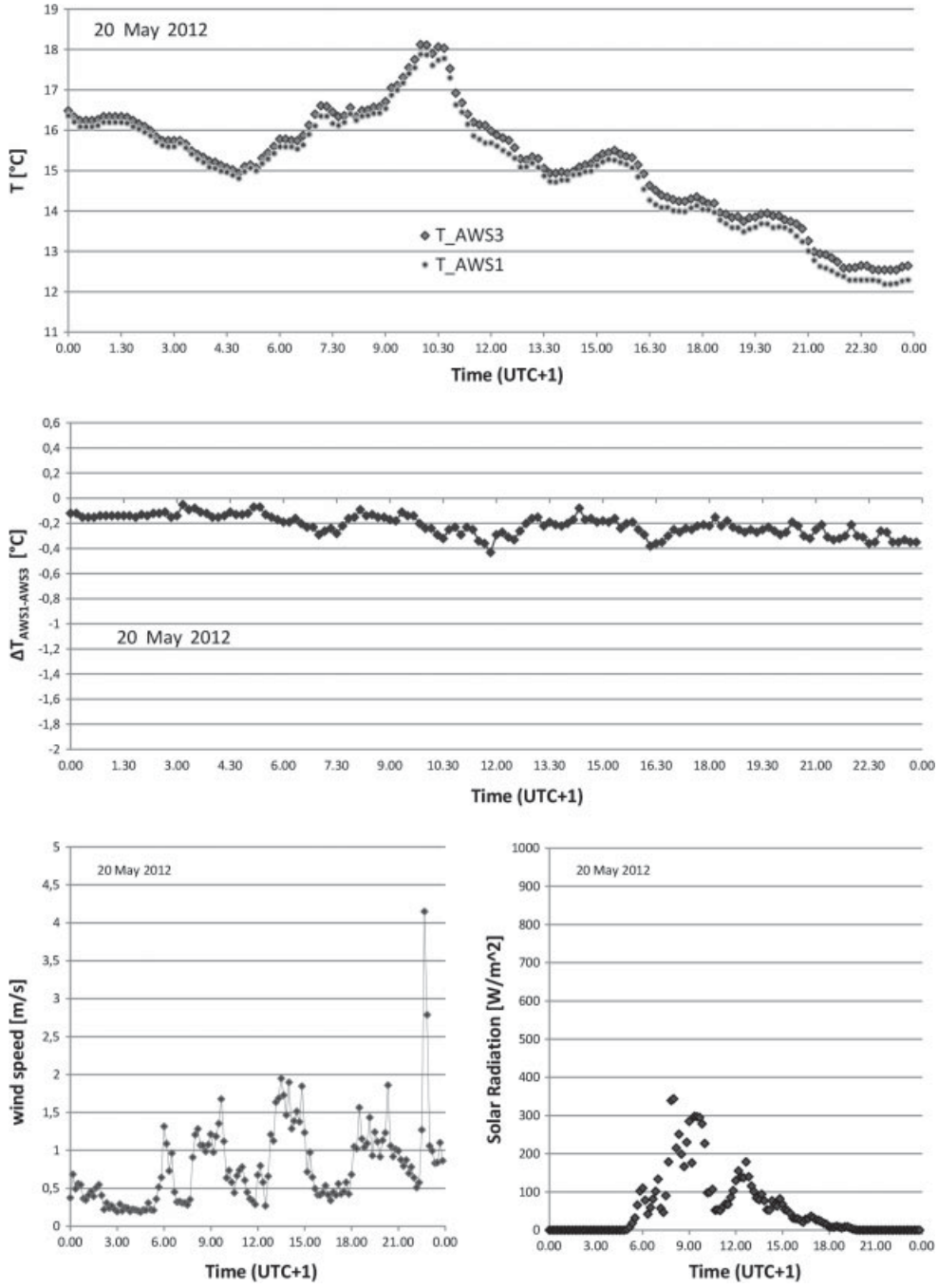

Figure 12. Temperature recorded by AWS1 and AWS3 for 20 May 2012. The figure also presents the temperature differences $\Delta T_{\mathrm{AWS1-AWS3}} = T_{\mathrm{AWS1}} - T_{\mathrm{AWS3}}$, wind speed, and solar radiation data.

These results show an evident increase in the heating of the AWS5 (respectively AWS3) screens due to the radiative contribution. The lower reflectivity of the screens causes the heating of the plates and a subsequent warming of the air inside, as it flows over the plates to the sensor. Obviously, this phenomenon is minimized in the new screens (AWS0 and AWS1) that more efficiently reflect the radiation thus better shielding the temperature sensor.

The presence of a radiative heating effect is confirmed also by the increase of temperature differences with increasing solar radiation and the decrease with increasing wind speed (Anderson and Baumgartner, 1998), as demonstrated in our observations.

The radiation incident on a shield surface is composed of two main components: solar radiation and thermal (infrared) radiation. Fuchs and Tanner (1965) investigated the performance of various shield coatings with respect to radiative characteristics for solar and thermal radiation (Fuchs and Tanner, 1965). In their work, they demonstrate that a good compromise should be reached (Hubbard et al., 2001) between solar absorptivity (a_s) to infrared absorptivity (a_t) and coatings with a small a_s/a_t

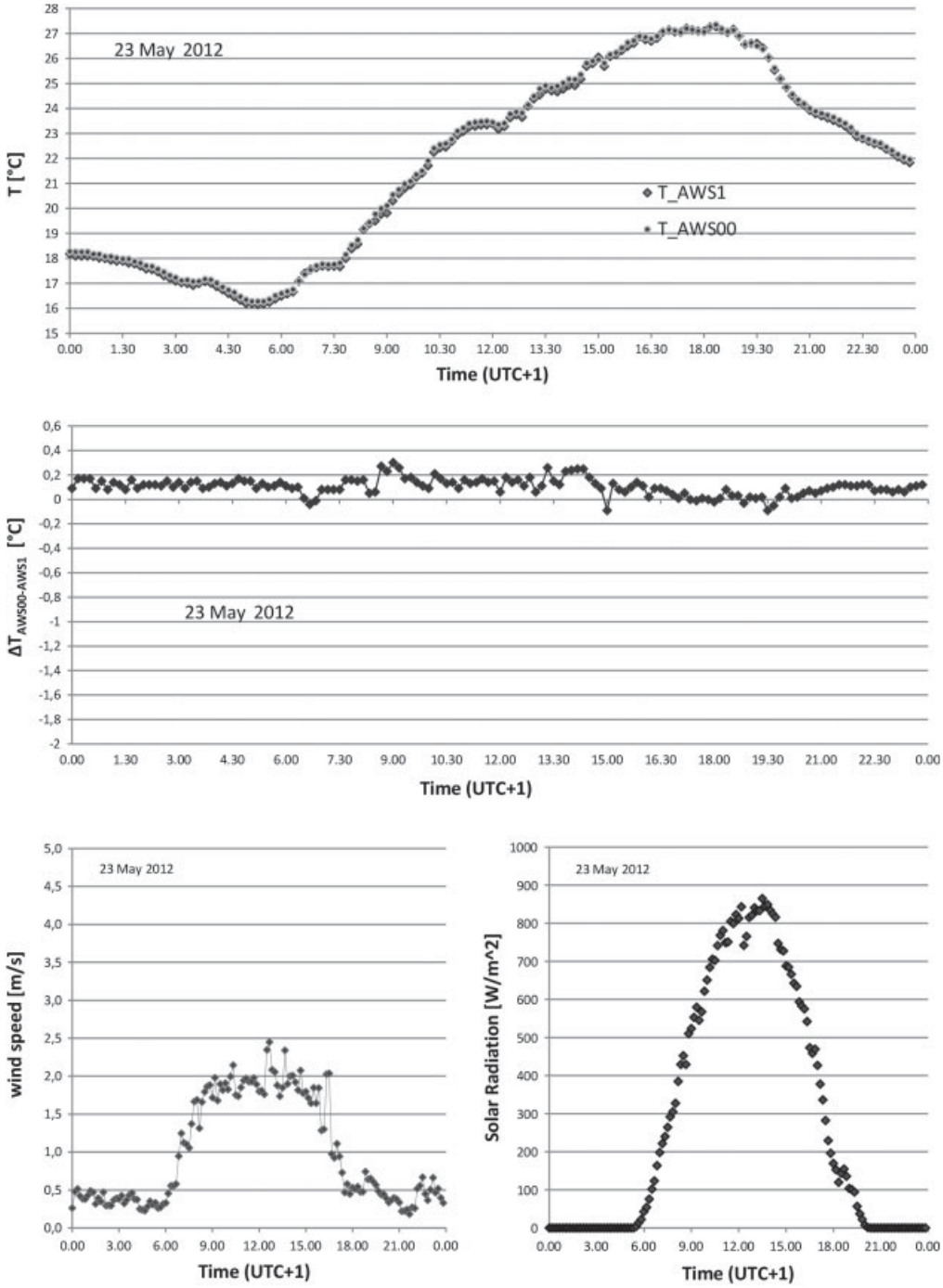

Figure 13. Temperature recorded by AWS00 and AWS1 for 23 May 2012. The figure also presents the temperature differences $\Delta T_{\mathrm{AWS00-AWS1}} = T_{\mathrm{AWS00}} - T_{\mathrm{AWS1}}$, wind speed, and solar radiation data.

ratio are best for solar radiation shields, particularly when they are resistant to weathering.

The results showed in this work can be explained following the Fuchs and Tanner's results. A raise of a_s/a_t ratio due to degradation of coating well explains the higher temperature measured by older screens.

Finally, we have experimentally demonstrated that screen ageing effects the temperature measurements introducing a source of error. The use of identical instrumentation at all sites is not sufficient to ensure comparable data. Consequently, the ageing process should be accounted for by means of a correction factor with its associated uncertainty or more generally when computing the total uncertainty budget of the daily temperature values. Further investigation on this correction and the associated uncertainty is required. Moreover, the effect and the associated correction depends on the shape, material, and coating of the shields, leading to dedicated evaluations for each model of manufactured shield. The ageing experiments illustrate in this work are therefore intended as a first attempt to obtain a further goal: improve the uncertainty budget evaluation in surface

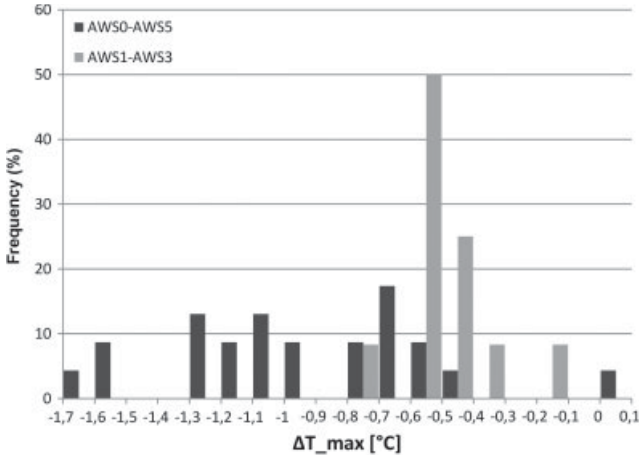

Figure 14. Histograms of the maximum differences recorded between AWS0 and AWS5 ($\Delta T^*_{AWS0-AWS5}$) in black and AWS1 and AWS3 ($\Delta T^*_{AWS1-AWS3}$) in grey.

air temperature measurements. A more comprehensive measurement uncertainty budget should include shield ageing effect but also different contribution as: siting, shield effectiveness (related to type, geometry, material, natural or artificial ventilation, etc.), sensor calibration, sensor response time, and so on.

The bias associated with screen ageing should be evaluated especially in climate analysis where long temperature data series are considered. The development of a temperature correction model keeping in to account this effect could be useful for climate studies. This preliminary work points to focus the attention of data users on drift in temperature due to shield, giving experimental evidence of the effect and its dependence from wind and solar radiation. A long-term comparison of different screens and the development of a temperature correction model for evaluating the ageing effect (in function of AWS working time, solar and weather exposure conditions, type of screen, etc.) are in progress in the framework of the MeteoMet Project (www.meteomet.org) aiming to assure meteorological traceability of atmospheric measurements.

Acknowledgements

These works are being developed within the frame of the EMRP, the EMRP is jointly funded by the EMRP participating countries within EURAMET and the European Union. Dr Paolo Allasia and Dr Giorgio Lollino–Consiglio Nazionale delle Ricerche, Istituto di Ricerca per la Protezione Idrogeologica–for providing solar irradiance and wind speed data.

References

Anderson SP, Baumgartner MF. 1998. Radiative Heating errors in naturally ventilated air temperature measurements made from buoys. *Journal of Atmospheric and Oceanic Technology* **15**: 157–173. 1520-0426.

Aoshima T, Nakashima K, Kawamura H ,Kumamoto M, Sakai T, Kawano S, Joko M. 2010. RIC-Tsukuba (Japan) Intercomparison of Thermometer Screens/Shields in 2009–2010. In *Paper presented at the WMO Technical Conference on Meteorological and Environmental Instruments and Methods of Observation* (TECO-2010), Helsinki, Finland, 30 August–1 September 2010.

BIPM, IEC, IFCC, ILAC, IUPAC, IUPAP, ISO, OIML. 2008. Evaluation of measurement data — guide for the expression of uncertainty in measurement. JCGM 100:2008. www.bipm.org/en/publications/guides/gum.html

Brandsma T, Van der Meulen JP. 2008. Thermometer screen intercomparison in De Bilt (the Netherlands)–Part II: description and modeling of mean temperature differences and extremes. *International Journal of Climatology* **28**: 389–400, DOI: 10.1002/joc.1524

Brunet M, Asin J, Sigrò J, Banon GF, Aguilar E, Palenzuela JE, Petersong TC, Jones P. 2011. The minimization of the screen bias from ancient Western Mediterranean air temperature records: an exploratory statistical analysis. *International Journal of Climatology* **31**: 1879–1895, DOI: 10.1002/joc.2192

Curci S, Virlan M, Lavecchia C. 2011. Traceability and reliability on meteorological measures: Policy management and data archiving from a network of homogeneous meteorological stations distributed on the national territory. In *Papers presented at the IEEE Workshop on Environmental Energy and Structural Monitoring Systems* (EESMS), Milano, Italy, 28 September 2011.

Fuchs M, Tanner CB. 1965. Radiation shields for air temperature thermometers. *Journal of Applied Meteorology* **4**: 544–547. 0021-8952.

Hubbard KG, Lin X, Walter-Shea EA. 2001. The Effectiveness of the ASOS, MMTS, Gill, and CRS Air Temperature Radiation Shields. *Journal of Atmospheric and Oceanic Technology* **18**: 851–864. 1520-0426.

Meda A, Merlone A, Pennecchi FR, Sardi M. 2009. Weather measurements traceability: an example at INRiM. *Measurement* **42**: 1482–1486.

Van der Meulen JP, Brandsma T. 2008. Thermometer screen intercomparison in De Bilt (the Netherlands), Part I: Understanding the weather-dependent temperature differences. *International Journal of Climatology* **28**: 371–387. DOI: 10.1002/joc

World Meteorological Organization (WMO). 2008. *Guide to Meteorological Instruments and Methods of Observation (WMO-No. 8)*. WMO: Geneve.

